CHEMISTRY
A EUROPEAN JOURNAL

The Clusters $[M_a(ECp^*)_b]$ (M = Pd, Pt; E = Al, Ga, In): Structures, Fluxionality, and Ligand Exchange Reactions**

Tobias Steinke, Christian Gemel, Manuela Winter, and Roland A. Fischer*[a]

Abstract: The synthesis and structural characterization of the novel homoleptic cluster complexes $[Pd_2(GaCp^*)_2(\mu_2\text{-}GaCp^*)_3]$ (**1c**), $[Pd_3(GaCp^*)_4(\mu_2\text{-}GaCp^*)_4]$ (**2b**) and $[Pd_3(AlCp^*)_2(\mu_2\text{-}AlCp^*)_2(\mu_3\text{-}AlCp^*)_2]$ (**3**) ($Cp^* = C_5Me_5$) are presented. Furthermore, ligand exchange reactions of these cluster complexes are explored. In contrast to the electronically and sterically saturated complexes $[M(ECp^*)_4]$ (M = Ni, Pd, Pt), the new unsaturated analogues $[M_a(ER)_b]$ (E = Al, Ga, In) react with a variety of typical ligands (Cp*Al, CO, phosphines, isonitriles) to give new di- and tri-substituted compounds like $[Pt_2(GaCp^*)_2(\mu_2\text{-}AlCp^*)_3]$ (**1d**), $[PdPt(GaCp^*)(PPh_3)(\mu_2\text{-}GaCp^*)_3]$ (**4b**), or $[Pd_3(PPh_3)_3(\mu_2\text{-}InCp^*)(\mu_3\text{-}InCp^*)_2]$ (**8**). The trends of the reactivity of $[M_a(ER)_b]$ as well as their fluxional behavior in solution has been elucidated by NMR spectroscopy, resulting in a mechanistic rationale for the ligand exchange reactions as well as the fluxional processes.

Keywords: carbenoids · cluster compounds · fluxionality · Group 13 elements · transition metals

Introduction

Oligonuclear homoleptic cluster compounds of the type $[M_a(ER)_b]$ (in general: M = d-block metal; $b > a > 1$) have inspired further exploration of the coordination chemistry of E^IR (E = Al, Ga, In; R = Cp*, $C(SiMe_3)_3$, etc.) compounds.[1–3] Recently it has been demonstrated, that ECp* (E = Ga, In) is capable of stabilizing certain M_aE_b clusters (M = Pd, Pt). These new structures and compositions go beyond the previously known mononuclear homoleptic complexes ME_4 (M = Ni, Pd, Pt)[4–6] and the heteroleptic compounds of the general formula $[M_a(ER)_bL_x]$ (M = d-block metal), which contain strongly bound ligands (L) such as CO or Cp that limit their reactivities considerably.[1] However, the two compounds Pt_2Ga_5[7] and Pd_3In_8[8] remain to date the sole examples of the target clusters M_aE_b. One reason for this rarity probably relates to the remarkably high bond energy of the donor–acceptor $M{-}E^I$ bonds of 40–60 kcal mol^{-1}.[9,10] In addition, the low-valent E^IR ligands are easily oxidized to yield E^{III} species of various kinds: carbene-type reactions such as insertion into M–X bonds (X = halide, alkyl, etc.) and cycloaddition to unsaturated functional groups have to be taken into account.[11–13] Last but not least, association/dissociation equilibria of $(E^IR)_x$ in solution play a role. As a consequence of this situation, the synthesis of ME_n and M_aE_b in general is prone to kinetic control. Thus, the successful synthesis of M_aE_b is highly dependent on the conditions and the particular combination of the starting compounds $[ML_n]$ and E^IR. Nevertheless, a rational approach of stepwise cluster formation starting out from the monomeric building blocks ME_4 was successful for the dinuclear Pt_2Ga_5 and its trimetallic $PtPdGa_5$ analogue.[14] The ME_4 compounds are rather inert in most cases, especially against ligand substitution which would require a pre-dissociation of E^IR. We found that this reaction path cannot be activated without unspecific decomposition of the starting complexes. However, there are some indications that lower coordinated, electronically and sterically unsaturated species like $[Ni(AlCp^*)_3]$ may exist as short-lived intermediates during the formation of ME_4. These unsaturated species exhibit interesting reactivity including activation of aromatic

[a] T. Steinke, C. Gemel, M. Winter, Prof. R. A. Fischer
Anorganische Chemie II—Organometallics & Materials
Ruhr-Universität Bochum, 44780 Bochum (Germany)
Fax: (+49) 234-321-4174
E-mail: roland.fischer@ruhr-uni-bochum.de

[**] Organo Group 13 Complexes of Transition Metals, Part 35; for Part 34 see ref. [34]. Complexes of the type $[M_a(ECp^*)_b]$ will be denoted M_aE_b throughout this article. Thus, Pt_2Ga_5 would mean $[Pt_2(GaCp^*)_5]$ or Pd_3In_8 would mean $[Pd_3(InCp^*)_8]$, and so forth.

Supporting information for this article is available on the WWW under http://www.chemeurj.org or from the author. The molecular structure of **7**, and an illustration of the molecular structure of $[(dvds)(\mu_2\text{-}Cp^*Al)_2]$ as well as important bond lengths and angles.

DOI: 10.1002/chem.200400959

C–H bonds under very mild conditions.[15] Key questions of the chemistry of mononuclear ME_n and oligonuclear M_aE_b compounds include: what is the range of M, E, *n*, *a*, and *b* of such compounds, being accessible in preparative yields? How about higher ($n=5, 6\ldots$) and lower ($n=2, 3$) coordination numbers at the center M? Will it be possible to derive giant clusters M_aE_b with $a, b \gg 1$ that exhibit a cluster core of M_a stabilized by a shell of surface bound E^IR ligands, such as in the case of the classical, giant carbonyl-metallate clusters $[M_a(CO)_b]^{m-}$ (M = Os, Pd, Pt, etc.)? At least, Schnöckel's fascinating, large aluminum cluster $[Al_{38}(AlCp^*)_{12}]$ points in that direction.[16] Table 1 lists all known homoleptic compounds M_aE_b (M = d-block metal), including the results of this work, indicating that this chemistry is still limited to the Group 10 metals Ni, Pd, Pt.

Table 1. Homoleptic cluster compounds of the type $[M_a(ECp^*)_b]$.

Compound	M:E	reference
monomeric		
$[Ni\{GaC(SiMe_3)_3\}_4]$	1:4	[17]
$[Ni\{InC(SiMe_3)_3\}_4]$	1:4	[4]
$[Pd\{InC(SiMe_3)_3\}_4]$	1:4	[14]
$[Pt\{InC(SiMe_3)_3\}_4]$	1:4	[5]
$[Ni(GaCp^*)_4]$	1:4	[6]
$[Pd(GaCp^*)_4]$	1:4	[14]
$[Pt(GaCp^*)_4]$	1:4	[14]
$[Ni(AlCp^*)_4]$	1:4	[15]
$[Pd(AlCp^*)_4]$	1:4	this work
$[Ni(AlCp^*)_3(GaCp^*)]$	1:4	[15]
dimeric		
$[Pt_2(GaCp^*)_2(\mu_2\text{-}GaCp^*)_3]$	2:5	[7]
$[PtPd(GaCp^*)_2(\mu_2\text{-}GaCp^*)_3]$	2:5	[14]
$[Pd_2(GaCp^*)_2(\mu_2\text{-}GaCp^*)_3]$	2:5	this work
$[Pd_2(AlCp^*)_2(\mu_2\text{-}AlCp^*)_3]$	2:5	this work
$[Pt_2(GaCp^*)_2(\mu_2\text{-}AlCp^*)_3]$	2:5	this work
trimeric		
$[Pd_3(InCp^*)_4(\mu_2\text{-}InCp^*)_4]$	3:8	[8]
$[Pd_3(GaCp^*)_4(\mu_2\text{-}GaCp^*)_4]$	3:8	this work
$[Pd_3(AlCp^*)_2(\mu_2\text{-}AlCp^*)_2(\mu_3\text{-}AlCp^*)_2]$	3:6	this work

Results

Reaction of $[Pd_2(dvds)_3]$ with ECp*: The reaction of $[Pd_2(dvds)_3]$ (dvds = 1,3-divinyl-1,1,3,3-tetramethyldisiloxane) with excess GaCp* is a vivid example of the subtle influence of the reaction conditions on M_aE_b cluster formation. At −30 °C in hexane the reaction yields the dinuclear compound $[Pd_2(GaCp^*)_2(\mu_2\text{-}GaCp^*)_3]$ (**1c**) in quantitative yield (Scheme 1). Only trace amounts (< 3 %) of monomeric $PdGa_4$ are observed. In contrast, the reaction conducted in toluene at 25 °C yields trinuclear $[Pd_3(GaCp^*)_4(\mu_2\text{-}GaCp^*)_4]$ (**2b**) in high yield. The dimeric species **1c** is formed only in insignificant amounts (< 2 %), and the $PdGa_4$ product is not detected at all. The related reaction of $[Pd_2(dvds)_3]$ with an excess of InCp* in hexane with gentle heating (50 °C) leads to the known trinuclear compound $[Pd_3(InCp^*)_8]$ (**2a**) in almost quantitative yield. On treatment of $[Pd_2(dvds)_3]$ with an excess of AlCp* in benzene at 60 °C, the trinuclear compound $[Pd_3(AlCp^*)_2(\mu_2\text{-}AlCp^*)_2(\mu_3\text{-}AlCp^*)_2]$ (**3**) is formed with a 3:6 rather than a 3:8 composition for *a*:*b* as in the two related above-mentioned cases. Compound **3** was obtained from saturated solutions of the sample in toluene as octahedral shaped deep red-brown single crystals in reproducible yields of 60 %.

Interestingly, the monomeric $PdGa_4$, which is quantitatively available by reaction of $[Pd(tmeda)Me_2]$ and GaCp*,[14] is

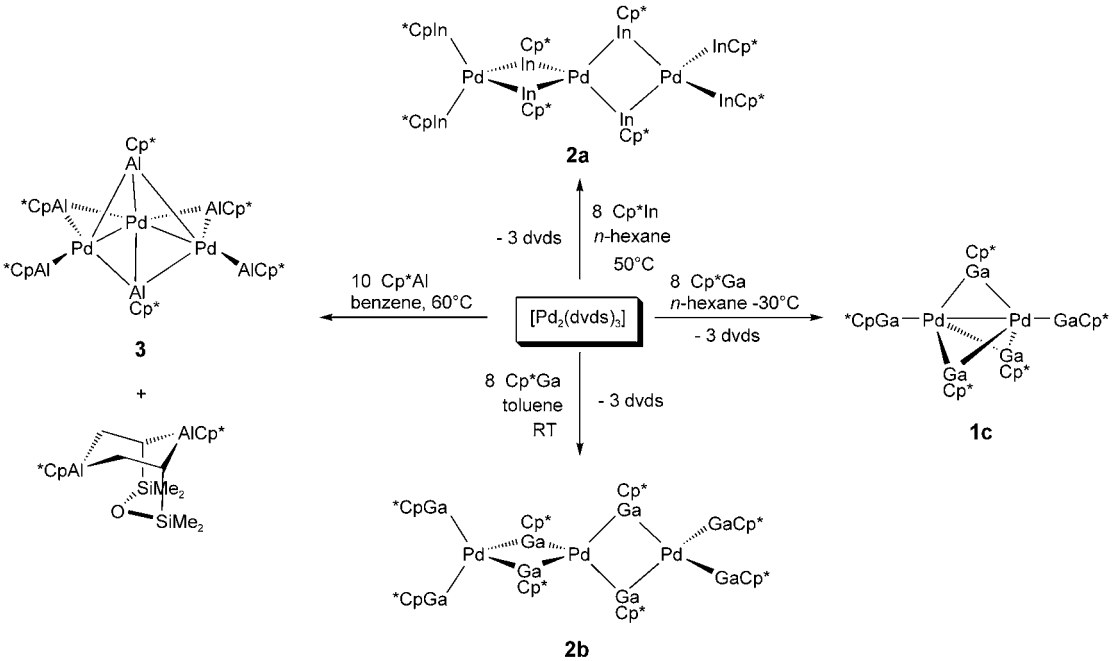

Scheme 1. Reactions of $[Pd_2(dvds)_3]$ with ECp*.

not formed by reaction of either **1c** or **2b** with an excess of the ligand. These observations are consistent with the remarkable inertness of the homologous trinuclear Pd_3In_8 (**2a**) against ligand addition and formation of three equivalents of $PdIn_4$.[8]

The Pd_2Ga_5 complex **1c** crystallizes in the triclinic space group $P\bar{1}$. Figure 1 shows a general illustration of M_2E_5 type

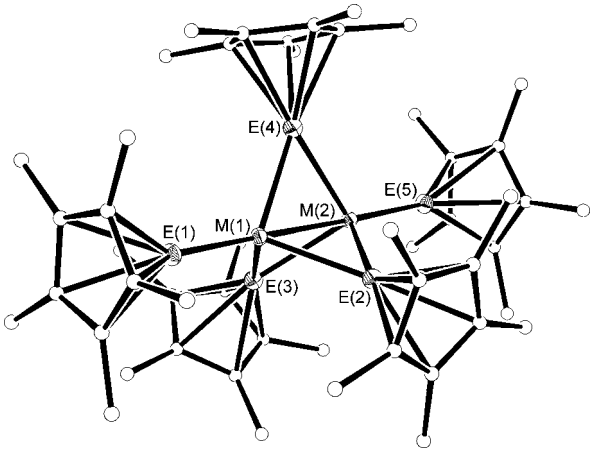

Figure 1. Molecular structure of $[M_2(ECp^*)_2(\mu_2\text{-}ECp^*)_3]$ (M = Pd, Pt; E = Al, Ga) in the solid state (Ortep drawing, 30% level of probability for the metal atoms, carbon atoms displayed as spheres for clarity).

clusters. The molecular structure of **1c** consists of a central Pd_2 unit with a somewhat short Pd–Pd distance of 2.6091(12) Å. In comparison, the tetranuclear cluster $[Pd_4(CO)_5(PPh_3)_4]$ exhibits a Pd–Pd bond length of 2.75–2.77 Å being regarded as bonding, whereas the nonbonding Pd–Pd bond length in the same molecule is 3.21 Å. Quantum chemical analyses of the Pt–Pt bond in the analogous Pt_2Ga_5 complex **1a** with the help of natural bond orbital (NBO) and atoms-in-molecules (AIM) methods suggests only weak d^{10}–d^{10} interactions.[7] The Pd_2 unit of **1c** is surrounded by two terminal and three bridging GaCp* ligands, resulting in a dipalladium-centered trigonal-bipyramidal structure (idealized D_{3h} symmetry). The terminal Pd–Ga bond lengths in **1c** (2.3583(14) and 2.3624(14) Å) are similar to the Pd–Ga bond length in $PdGa_4$ (2.3668(7) Å), while the bridging Pd–Ga bond lengths are distinctly longer (2.4867(14)–2.5052(14) Å). All Cp* moieties are bound to the Ga centers in a nearly ideal symmetric η^5 mode with average values for the $Cp^*_{centroid}$–Ga bond lengths of 1.999 Å for the terminal Cp*Ga units and 2.048 Å for the bridging ligands, both values being close to the free ligand value of 2.081 Å (gas phase, monomer).[18]

The NMR spectra of the dinuclear Pd_2Ga_5 (**1c**) in C_6D_6 exhibit only one set of signals for the GaCp* ligands (^{1}H: $\delta = 1.98$ ppm; ^{13}C: $\delta = 113.3$ and 10.8 ppm), that is, a fluxional process is active, exchanging the bridging and terminally coordinated ligands on the NMR timescale. At −80 °C in [D_8]toluene the signal splits into two distinguishable resonances (2.07 and 2.03 ppm) with an integral ratio of 2:3 accounting for a structure similar to that observed in the solid state. The corresponding complex Pt_2Ga_5 (**1a**) shows a static spectrum at room temperature.

The Pd_3Ga_8 complex **2b** crystallizes in the monoclinic space group $C2/c$. The molecular structure (Figure 2) is very similar, but not isostructural to the analogous indium com-

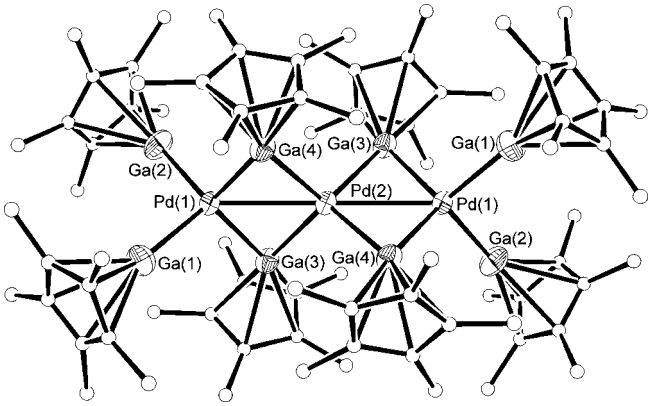

Figure 2. Molecular structure of $[Pd_3(GaCp^*)_4(\mu_2\text{-}GaCp^*)_4]$ (**2b**) in the solid state (Ortep drawing, 50% level of probability for the metal atoms, carbon atoms displayed as spheres for clarity).

Table 2. Selected bond lengths [Å] and angles [°] for **2b**.[a]

Pd(1)–Pd(2)	2.843(5)	Cp*–Ga(3)	2.064
Pd(1)–Ga(1)	2.399(3)	Cp*–Ga(4)	2.060
Pd(1)–Ga(2)	2.418(3)	Pd(1)-Pd(2)-Pd(3)	179.53(4)
Pd(1)–Ga(3)	2.442(3)	Ga(1)-Pd(1)-Ga(2)	105.09(13)
Pd(1)–Ga(4)	2.448(3)	Ga(3)-Pd(1)-Ga(4)	112.16(13)
Pd(2)–Ga(3)	2.514(3)	Ga(1)-Pd(1)-Ga(3)	109.41(15)
Pd(2)–Ga(4)	2.517(3)	Cp*-Ga(1)-Pd(1)	175.30
Cp*–Ga(1)	2.046	Cp*-Ga(2)-Pd(1)	168.86
Cp*–Ga(2)	2.069	Ga(3)-Pd(1)-Pd(2)-Ga(4)	174.18(4)

[a] Cp* values are taken from the centroid of the Cp* moiety.

pound Pd_3In_8 (**2a**).[8] The three central palladium atoms are linearly arranged (179.53(4)°; Table 2). The Ga-Pd-Ga angles are slightly smaller than the ideal tetrahedral angle of 109° for the terminal Ga atoms (105.09°) and slightly larger for the bridging Ga atoms (112.16(13)°). Correspondingly, the dihedral angle Ga(3)-Pd(1)-Pd(2)-Ga(4) deviates from planarity only by 5.82(4)°. The terminal Pd–Ga bond lengths (2.399(3) and 2.418(3) Å) are shorter than the bridging ones (2.442(3) and 2.448(3) Å), while the Pd–Ga bond lengths around the central palladium atom are the longest (about 2.51 Å). The $Cp^*_{centroid}$–Ga bond lengths have values in the range of 2.046–2.069 Å.

The ^{1}H NMR spectrum of Pd_3Ga_8 (**2b**) in C_6D_6 at room temperature exhibits two resonances at $\delta = 2.05$ and 1.96 ppm with an integral ratio of 1:3. This unexpected integral ratio, if compared with the solid-state structure, was also observed in the NMR spectrum of the analogous Pd_3In_8 species **2a**, yet only at low temperatures (−80 °C). At higher temperatures (+80 °C) compound **2b** shows only one coalesced signal; the same was observed for **2a** at room temperature.

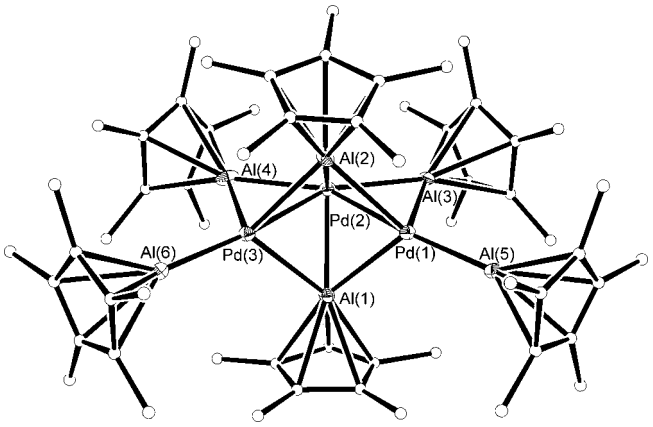

Figure 3. Molecular structure of $[Pd_3(AlCp^*)_2(\mu_2\text{-}AlCp^*)_2(\mu_3\text{-}AlCp^*)_2]$ (**3**) in the solid state (Ortep drawing, 30% level of probability for the metal atoms, carbon atoms displayed as spheres for clarity).

The molecular structure of Pd_3Al_6 (**3**) is depicted in Figure 3 and exhibits a Pd_3 triangle coordinated by two perpendicular (axial) μ_3-bridging and four equatorial AlCp* ligands (two μ_2-bridging and two terminal). The three central palladium atoms are arranged with an angle Pd(3)-Pd(2)-Pd(1) of 87.13(6)° (Table 3). The longest Pd–Pd distance of 3.619 Å (Pd(1)–Pd(3)) can be regarded as nonbonding, while the other two Pd–Pd bond lengths of 2.6157(18) and 2.6363(19) Å are shortened due to the edge-bridging AlCp* ligands. These Pd–Pd bond lengths are distinctly shorter than in **2a** or **2b**. Both faces of the metal triangle are capped by a μ_3-AlCp* unit (Al(1) and Al(2)). The μ_3-Al–μ_3-Al vector does not intersect the center of symmetry of the Pd_3 triangle, but is rather shifted towards the Pd(1)–Pd(3) axis, forming an almost planar Pd(1)-Al(1)-Pd(3)-Al(2) square (9.3° deviation). The Pd(1,3)–Al(1,2) bond lengths are in the range 2.561(5)–2.601(5) Å, while the Pd(2)–Al(1,2) bonds are shorter (2.478(5)–2.498(5) Å). The equatorial μ_2-AlCp* units are arranged almost in plane to the Pd_3 triangle and also are somewhat closer to the central Pd(2) center. As expected, the shortest Pd–Al bond lengths are found for the terminally coordinated AlCp* units with an average value of 2.373 Å. These terminal units are coordinated in the plane of the Pd_3 core with deviations of 6.3° and 0.6°. The $Cp^*_{centroid}$–Al bond lengths have values in the range 1.919–2.003 Å (average 1.953 Å), showing no systematic differences between terminal and bridging ligands. These values are close to free AlCp* (gas phase: monomer, 2.015 Å)[19] and are distinctly longer than the distances in the metal carbonyl complexes $[(CO)_5Cr(AlCp^*)]$ (1.819 Å)[20] and $[(CO)_4Fe(AlCp^*)]$ (1.775 Å)[21] with significantly more polarized $M^{\delta-}$–$E^{\delta+}$ bonds.

Table 3. Selected bond lengths [Å] and angles [°] for **3**.[a]

Pd(1)–Pd(2)	2.6157(18)	Pd(1)-Pd(2)-Pd(3)	87.13(6)
Pd(2)–Pd(3)	2.6363(19)	Pd(1)-Al(1)-Pd(3)	89.18(16)
Pd(1)–Pd(3)	3.619(18)	Pd(1)-Al(2)-Pd(2)	61.93(12)
Pd(1)–Al(1)	2.592(5)	Pd(1)-Al(3)-Pd(2)	64.67(12)
Pd(2)–Al(1)	2.498(5)	Pd(2)-Pd(1)-Al(5)	173.15(14)
Pd(3)–Al(1)	2.563(5)	Al(5)-Pd(1)-Al(3)	117.12(18)
Pd(1)–Al(3)	2.488(5)	Al(5)-Pd(1)-Al(2)	127.42(17)
Pd(2)–Al(3)	2.401(5)	Al(3)-Pd(2)-Al(4)	154.76(17)
Pd(1)–Al(5)	2.369(5)	Cp*-Al(5)-Pd(1)	178.24
Cp*–Al(1)	1.959	Pd(1)-Pd(2)-Pd(3)-Al(1)	56.76(14)
Cp*–Al(3)	2.003	Pd(1)-Pd(2)-Pd(3)-Al(3)	178.38(15)
Cp*–Al(5)	1.919	Pd(1)-Pd(2)-Pd(3)-Al(5)	173.7(11)

[a] Cp* values are taken from the centroid of the Cp* moiety.

The ^{1}H NMR spectrum of **3** in C_6D_6 at room temperature exhibits two distinguishable singlets at $\delta = 2.05$ and 1.97 ppm with an integral ratio of 1:2. In the range +80 °C to −80 °C no changes of the NMR spectrum are observed, that is, neither broadening, decoalescence, nor coalescence of the signals. As an explanation for this observation, it is suggested, that the axially coordinated AlCp* ligands do not participate in the fluxional ligand-exchange process of the equatorial (terminal and edge-bridging) ligands on the NMR timescale.

As a stoichiometric side product in the formation of **3**, the colorless compound $[(dvds)(\mu_2\text{-}Cp^*Al)_2]$ is formed.[22] An illustration of the molecular structure of $[(dvds)(\mu_2\text{-}Cp^*Al)_2]$ as well as important bond lengths and angles are included in the Supporting Information.

Ligand exchange in the homoleptic dinuclear cluster complexes M_2Ga_5 (M = Pd, Pt): Treatment of the dinuclear Pt_2Ga_5 (**1a**) with AlCp* in toluene at +80 °C quantitatively leads to the partially exchanged compound $[Pt_2(GaCp^*)_2(\mu_2\text{-}AlCp^*)_3]$ (**1d**). In contrast, the reaction of the Pd analogue Pd_2Ga_5 (**1c**) gives the fully exchanged dinuclear compound $[Pd_2(AlCp^*)_2(\mu_2\text{-}AlCp^*)_3]$ (**1e**; Scheme 2). Attempts to synthesize the homoleptic complex Pt_2Al_5 from **1a** in the presence of excess AlCp* were not successful. ^{1}H NMR spectra of both **1d** and **1e** exhibit two signals at $\delta = 2.07/1.86$ ppm and $\delta = 2.00/1.94$ ppm, respectively, with the expected integral ratio of 2:3.

Compounds **1d** and **1e** are isostructural and crystallize in the monoclinic space group *C*2/*c*. The molecular structures are analogous to Pt_2Ga_5 (**1a**) and Pd_2Ga_5 (**1c**) with only minor deviations (Figure 1, Table 4). The AlCp* ligands in **1d** are solely located in the bridging positions.

It is worth noting that the substitution of InCp* by AlCp* or GaCp* is not restricted to the dinuclear systems. Thus, the reaction of Pd_3In_8 (**2a**) with stoichiometric amounts of GaCp* or AlCp leads to a substitution of the coordinated InCp* ligands as shown by in situ NMR experiments. However, the substitution reactions were incomplete, giving mixtures of insoluble trisubstituted complexes that could not be further characterized.

The reaction of M_2Ga_5 ($M_2 = Pt_2$ **1a**, PdPt **1b**, Pd_2 **1c**,) with PPh_3 in toluene yields the monosubstituted complexes $[MPt(GaCp^*)(PPh_3)(\mu_2\text{-}GaCp^*)_3]$ (M = Pt **4a**, Pd **4b**) and the disubstituted compound $[Pd_2(PPh_3)_2(\mu_2\text{-}GaCp^*)_3]$ (**5**), respectively (Scheme 2). The ^{1}H NMR spectrum of **4a** exhibits two singlets for the GaCp* units at $\delta = 2.12$ and 1.84 ppm with an integral ratio of 1:3. The ^{31}P{^{1}H} NMR resonance at

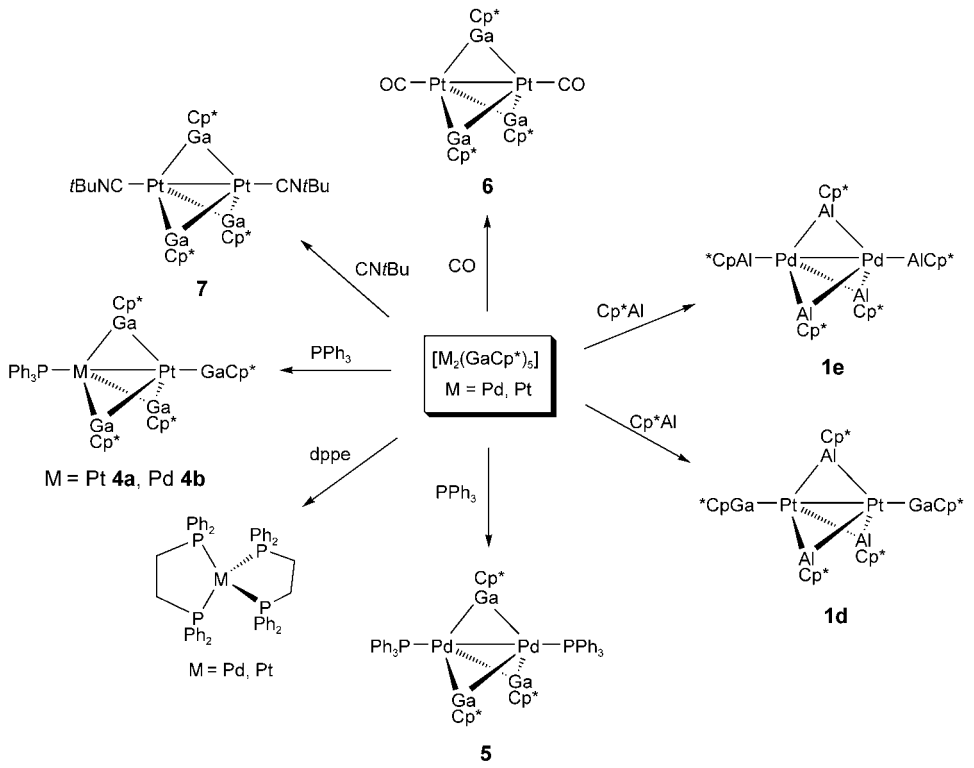

Scheme 2. Ligand exchange reactions of the homoleptic dinuclear cluster complexes $[M_2(GaCp^*)_5]$ (M = Pd, Pt).

disubstituted product **5** exhibits one set of signals for the bridging GaCp* units at $\delta =$ 1.77 ppm and signals for the phenyl groups at $\delta = 7.85$–7.05 ppm. The $^{31}P\{^1H\}$ NMR resonance is found at $\delta =$ 34.8 ppm. Monitoring this reaction by ^1H NMR spectroscopy reveals the monosubstituted complex $[Pd_2(GaCp^*)(PPh_3)(\mu_2\text{-}GaCp^*)_3]$ to be a reaction intermediate, giving rise to two singlets at $\delta = 2.12$ and 1.87 ppm with an integral ratio of 1:3. All attempts to isolate this intermediate failed.

The molecular structure of both **4a** and **4b** is depicted in Figure 4. Both compounds crystallize in the triclinic space group $P\bar{1}$. The molecular structure consists of a Pt_2 or a PdPt core, respectively, coordinated by one terminal PPh_3, one terminal GaCp* and three bridging GaCp* ligands, which basically represents the M_2E_5 structure type shown in Figure 1. The central P-M-Pt-Ga connectivity is almost linear. The phenyl rings coordinated at P(1) approximately occupy a staggered conformation with respect to the bridging GaCp* ligands. Due to steric repulsion between the PPh_3 group and the bridging GaCp* units, the angles M-P-C(phenyl) (average 116.65° for **4a** and 115.31° for **4b**, see Table 5) are

Table 4. Selected bond lengths [Å] and angles [°] for **1c**, **1d**, and **1e**.[a]

	Pd_2Ga_5 (**1c**)	$Pt_2Al_3Ga_2$ (**1d**)	Pd_2Al_5 (**1e**)
M(1)–M(2)	2.6091(12)	2.5585(3)	2.6327(11)
M(1)–E(1)	2.3624(14)	2.3310(7)	2.3230(18)
M(1)–E(2)	2.4945(15)	2.4259(16)	2.4559(18)
M(1)–E(3)	2.5052(14)	2.4237(17)	2.4559(18)
Cp*–E(1)	2.004	1.988	1.974
Cp*–E(2)	2.053	1.919	1.936
Cp*–E(3)	2.032	1.925	1.940
E(1)-M(1)-M(2)	177.44(5)	178.12(2)	179.00(5)
M(1)-E(2)-M(2)	63.17(4)	63.46(4)	65.01(5)
M(1)-M(2)-E(2)	58.56(3)	58.52(4)	57.26(5)
E(1)-M(1)-E(2)	119.51(5)	122.03(4)	121.84(7)
E(2)-M(1)-E(3)	92.90(5)	95.66(6)	94.83(5)
Cp*-E(1)-M(1)	178.77	177.38	176.69

[a] Cp* values are taken from the centroid of the Cp* moiety.

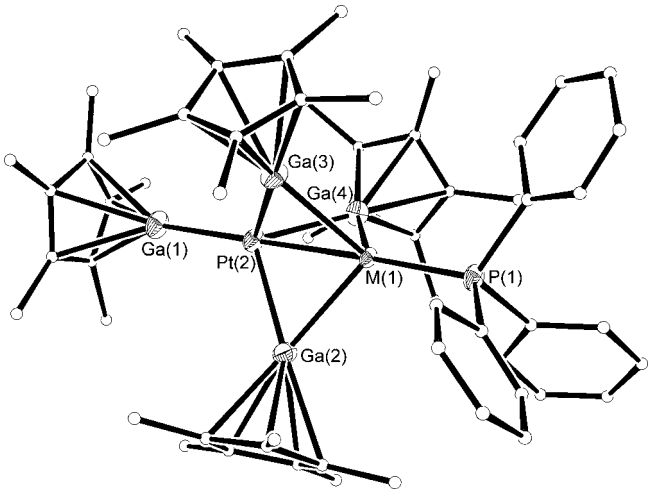

Figure 4. Molecular structure of $[MPt(GaCp^*)(PPh_3)(\mu_2\text{-}GaCp^*)_3]$ (M = Pt **4a**, Pd **4b**) in the solid state (Ortep drawing, 30% level of probability for the metal atoms, carbon atoms displayed as spheres for clarity).

$\delta = 66.0$ ppm shows the expected J(Pt,P) coupling (^1J(Pt,P) = 5685 Hz, ^2J(Pt,P) = 276 Hz). In the case of the trisubstituted compound **1b**, the substitution is observed only at the Pd center, leaving the Pt–GaCp* bond unchanged, as shown by the $^{31}P\{^1H\}$ resonance at $\delta = 53.0$ ppm with a significantly small ^2J(Pt,P) coupling of 494 Hz.

In contrast to the rather slow substitution reaction of **1a**, the reaction of **1c** with PPh_3 takes place at lower temperatures (RT) quantitatively with a shorter reaction time (< 1 h). Both terminally coordinated GaCp* ligands in **1c** are readily replaced by PPh_3 at room temperature, giving **5** in almost quantitative yields. The ^1H NMR spectrum of the

Table 5. Selected bond lengths [Å] and angles [°] for **4a** and **4b**.[a]

	$Pt_2Ga_4(PPh_3)$ (**4a**)	$PdPtGa_4(PPh_3)$ (**4b**)
M(1)–Pt(2)	2.6008(10)	2.5888(10)
M(1)–P(1)	2.242(3)	2.242(3)
Pt(2)–Ga(1)	2.3379(15)	2.3513(17)
M(1)–Ga(2)	2.5226(17)	2.4966(18)
Pt(2)–Ga(2)	2.4459(17)	2.4589(18)
Cp*–Ga(1)	1.976	1.974
Cp*–Ga(2)	2.019	2.007
P(1)–C	1.825(12)–1.844(13)	1.794(16)–1.839(13)
Ga(1)-Pt(2)-M(1)	179.29(5)	179.31(5)
P(1)-M(1)-Pt(2)	177.20(8)	177.58(9)
M(1)-Ga(2)-Pt(2)	63.11(4)	62.98(5)
M(1)-P(1)-C	114.8(5)–118.0(4)	113.2(6)–117.5(5)
C-P(1)-C	100.3(6)–102.2(6)	102.4(6)–103.6(7)
Cp*-Pt(2)-M(1)	179.30	178.72
C-P(1)-M(1)-Ga[b]	48.5(5)–71.5(5)	48.5(5)–73.0(6)

[a] Cp* values are taken from the centroid of the Cp* moiety; carbon atoms are from the phenyl group. [b] This describes the dihedral angles between the C atoms attached to the phosphorus and the bridging Ga units.

bigger than 109°, while the angles C(phenyl)-P-C(phenyl) (average 101.43° for **4a** and 103.00° for **4b**) are smaller than 109°. Similar distortions have been observed in the complex $[Pd(PPh_3)_3]$ (Pd-P-C(phenyl) 114.71–124.92°; C(phenyl)-P-C(phenyl) 99.83–102.27°).[23] The $Cp^*_{centroid}$–Ga bond lengths for the bridging GaCp* units (average 2.021 Å for **4a** and 2.006 Å for **4b**) and the terminal ligands (1.976 Å for **4a** and 1.974 Å for **4b**) are almost equal to that found for the $Cp^*_{centroid}$–Ga bond in **1a** or **1c**. Also the Pt–Pt bond length of 2.589(1) Å in **4a** is not significantly different from the metal–metal distance in **1a**. The Pd–Pt bond length in **4b** has a value of 2.601(1) Å.

Monomeric complexes of the type $[M(GaCp^*)_{4-x}(PPh_3)_x]$ ($x = 1$–4) were not formed as side products in the reactions yielding **4** and **5**. However, when the chelating diphosphine ligand dppe (dppe = bis(diphenylphosphinoethane)) is treated with M_2Ga_5, all GaCp* units are cleaved and the monomeric complexes $[M(dppe)_2]$ (M = Pd, Pt) are quantitatively obtained (Scheme 2). It was not possible to selectively derive complexes of the type $[M(ER)_2(L_2)]$ with L_2 being a chelating phosphane. However, compounds of that kind do exist, for example, $[Pt(ECp^*)_2(dcpe)]$ (dcpe = bis(dicyclohexylphosphino)ethane), and were synthesized by trapping the in situ formed $[L_2Pt]$ with stoichiometric amounts of ECp*.[24,25]

In the presence of stronger π-acceptor ligands the dinuclear molecular structure M_2Ga_3 is retained and disubstituted species similar to **5** are formed. Thus, the reaction of Pt_2Ga_5 with an excess of CO or CN*t*Bu yields the complexes $[Pt_2(CO)_2(\mu_2\text{-}GaCp^*)_3]$ (**6**) and $[Pt_2(CNtBu)_2(\mu_2\text{-}GaCp^*)_3]$ (**7**), respectively (Scheme 2). The formation of **6** could only be confirmed in situ by NMR and IR spectroscopy, as the complex is apparently stable only under an atmosphere of CO gas. The precipitation of trace amounts of a black solid in the absence of CO points to the formation of metallic platinum as a decomposition product. The ^{1}H NMR spectrum of **1a** in an atmosphere of CO in C_6D_6 shows one resonance for the three coordinated GaCp* ligands at $\delta =$ 1.85 ppm and a singlet for the uncoordinated GaCp* units ($\delta = 1.92$ ppm) in a ratio of 3:2. In accordance with the substitution reactions of M_2E_5 with PR_3 described above, a substitution of the terminal GaCp* units to CO is assumed. No exchange of free to coordinated ligand is observed on the NMR timescale. The coordinated CO gives rise to a ^{13}C resonance at $\delta = 209.6$ ppm. The solution IR spectrum of **6** reveals one sharp absorption at 1962 cm^{-1} in the region typical for terminally bound CO. Complex **7** was characterized by means of NMR spectroscopy, elemental analysis, and single-crystal X-ray analysis. The determined molecular structure of **7** shows no unexpected features and will not be discussed herein (see Supporting Information). The ^{1}H NMR spectrum exhibits one singlet at $\delta = 2.06$ ppm for the GaCp* units and one resonance at $\delta = 1.13$ ppm for the two *t*BuNC groups in a ratio of about 45:18. By monitoring the formation of **7** by ^{1}H NMR spectroscopy, the monosubstituted product can be detected, exhibiting two singlets at $\delta = 2.05$ and 1.98 ppm with an integral ratio for the terminal and bridging GaCp* moieties of 1:3 and one resonance at $\delta =$ 1.17 ppm representing the *t*BuNC ligand.

Ligand exchange reactions in the homoleptic cluster complex Pd_3In_8: Corresponding to the substitution reactions of M_2E_5 described above, the reaction of the trinuclear compound **2a** with PPh_3 or dppe proceeds by retaining the Pd_3 core. However, the linear arrangement of the transition metals in the solid state is not sustained: the two triangular Pd_3 clusters $[Pd_3(PPh_3)_3(\mu_2\text{-}InCp^*)(\mu_3\text{-}InCp^*)_2]$ (**8**) and $[Pd_3(dppe)_2(\mu_2\text{-}InCp^*)(\mu_3\text{-}InCp^*)_2]$ (**9**) were isolated (Scheme 3).

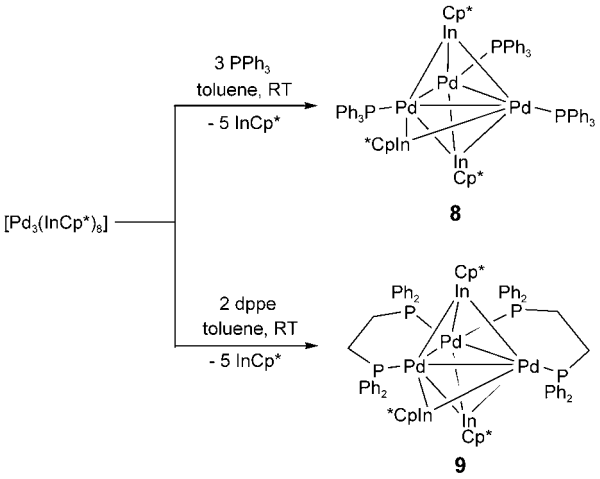

Scheme 3. Synthesis of $[Pd_3(InCp^*)_3(PPh_3)_3]$ (**8**) and $[Pd_3(InCp^*)_3(dppe)_2]$ (**9**).

Both complexes were characterized by means of NMR spectroscopy, elemental analysis, and single-crystal X-ray analysis. The key features of the molecular structures of **8** and **9** are almost identical, hence only the structure of **8** is briefly discussed (Figure 5).

The molecular structure of **8** consists of a triangular Pd_3 core, both faces of the metal triangle being capped by two

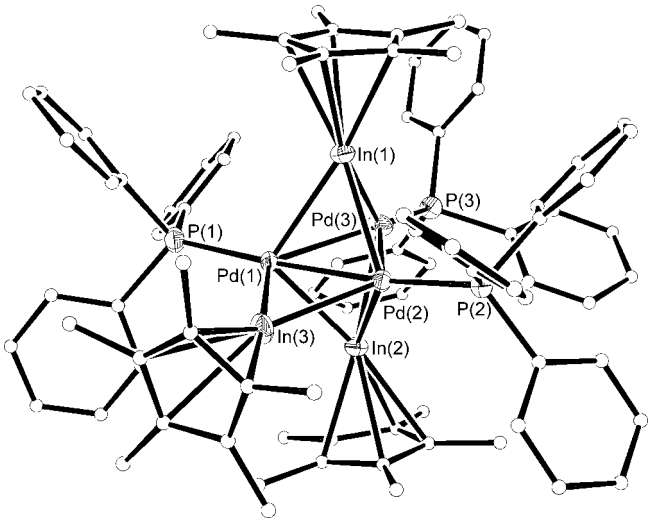

Figure 5. Molecular structure of $[Pd_3(InCp^*)_3(PPh_3)_3]$ (**8**) in the solid state (Ortep drawing, 30% level of probability for the metal atoms, carbon atoms displayed as spheres for clarity).

InCp* units, resulting in a slightly distorted trigonal bipyramidal geometry. The third InCp* ligand (In(3)) is found in μ_2-coordination mode almost parallel to the Pd_3 plane (deviation 6.9°). Additionally, each Pd center is coordinated by one PPh_3 ligand. The Pd–Pd bond lengths in **8** have values of 2.6283(11) Å (Pd(1)–Pd(2)), 2.9306(17) Å (Pd(2)–Pd(3)), and 2.8003(17) Å (Pd(1)–Pd(3))(Table 6). The short Pd(1)–Pd(2) bond length is possibly a result of the μ_2-bridging In(3)Cp* ligand. The Pd–In bond lengths of the μ_3-bridging InCp* moieties have average values of 2.7068 Å (In(1)) and 2.6830 Å (In(2)), the μ_3-InCp* units being slightly shifted (5.3° and 13.0°) towards the Pd(3) center.

Table 6. Selected bond lengths [Å] and angles [°] for **8**.[a]

Pd(1)–Pd(2)	2.6283(11)	Cp*–In(1)	2.262
Pd(1)–Pd(3)	2.8003(17)	Cp*–In(2)	2.235
Pd(2)–Pd(3)	2.9306(17)	Cp*–In(3)	2.299
Pd(1)–In(3)	2.6447(15)	Pd(1)-Pd(2)-Pd(3)	60.20(4)
Pd(2)–In(3)	2.7094(15)	Pd(1)-Pd(3)-Pd(2)	54.54(4)
Pd(1)–In(1)	2.7325(10)	Pd(1)-In(3)-Pd(2)	58.78(4)
Pd(3)–In(1)	2.6597(14)	Pd(1)-In(1)-Pd(2)	57.54(3)
Pd(1)–In(2)	2.7235(12)	P(1)-Pd(1)-Pd(2)	174.89(7)
Pd(3)–In(2)	2.6183(12)	P(1)-Pd(1)-In(3)	116.54(8)
Pd(1)–P(1)	2.267(2)	Pd(1)-P(1)-C	114.2(3)–118.4(3)
Pd(2)–P(2)	2.278(2)	C-P(1)-C	100.8(4)–104.2(4)
Pd(3)–P(3)	2.255(3)	Pd(1)-Pd(2)-Pd(3)-In(3)	173.12(7)

[a] Cp* values are taken from the centroid of the Cp* moiety; carbon atoms are from the phenyl group.

The ^{1}H NMR spectrum of **8** in C_6D_6 exhibits two singlets for the InCp* units at $\delta = 2.11$ and 1.70 ppm in a ratio of 1:2 and signals for the PPh_3 ligand at $\delta = 7.85$–7.35 ppm. The $^{31}P\{^1H\}$ NMR shows two singlet resonances at $\delta = 30.3$ and 13.6 ppm with an intensity ratio of 2:1. The ^{1}H NMR spectrum of compound **9** is similar to **8** and shows no unusual features. The $^{31}P\{^1H\}$ NMR of **9** shows two equally intense triplet resonances at 28.4 ($^3J(P,P) = 24.3$ Hz) and 20.9 ppm ($^3J(P,P) = 24.6$ Hz).

Discussion

Fluxionality of homoleptic clusters M_aE_b: Taking into account that Pt_2Ga_5 (**1a**) and Pd_2Al_5 (**1e**) give static spectra, whereas Pd_2Ga_5 (**1c**) gives only one coalesced signal at room temperature, a qualitative trend for the relative rates of the ligand-exchange processes can be estimated as being: Pt_2Ga_5 (**1a**) $\approx Pd_2Al_5$ (**1e**) $< Pd_2Ga_5$ (**1c**). This is in good agreement with the calculated M–E bond energies in the monomeric compounds $[M\{E(CH_3)\}_4]$ (M = Ni, Pd, Pt; E = B–Tl), which have the order Ni ≈ Pt > Pd for the transition metals, while for the Group 13 elements the trend B > Al > Ga ≈ In > Tl is found.[9,10,17] These results are also consistent with the NMR spectrum of the trisubstituted compound **1b**, for which only "half" of the fluxional process at room temperature on one of the two cluster core atoms is observed. Most likely, the Pd–Ga bond in **1b** is weaker than the Pt–Ga bond resulting in a fast exchange of bridging versus terminal ligands on the Pt center (vide infra).[14]

A similar trend is found in the trinuclear homoleptic series Pd_3E_8. While Pd_3Ga_8 (**2b**) exhibits two resonances at room temperature, the corresponding Pd_3In_8 species (**2a**), shows decoalescence only at −80 °C. This difference matches qualitatively with the decreasing order of the bond energies M–E for the heavier element E. The reason for the unusual ratio of 1:3 of the decoalesced peaks is uncertain and is not in agreement with the solid-state structure. A dissociation of the trinuclear component into two $Pd(ECp^*)_3$ fragments and one $Pd(ECp^*)_2$ (E = Ga, In) unit can not be excluded on the basis of the spectroscopic data, yet the reactivity of Pd_3In_8 (**2a**) with phosphines (PPh_3 or dppe) suggests that the nuclearity is retained in solution. A dissociation of Pd_3E_8 into Pd_3E_6 and two ECp* units is unlikely and can be excluded on the basis of ^{1}H NMR chemical shifts. Remember that the saturated homoleptic compounds also do not show dissociative equilibria. Scheme 4 presents a speculative

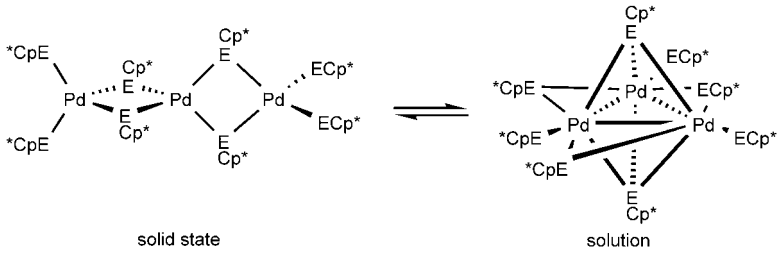

Scheme 4. Proposed interconversion between solution and solid-state structures of Pd_3E_8 (E = Ga, In).

mechanism for the interconversion of linear to triangular clusters of Pd_3E_8 in solution, bearing two axial and six equatorial ligands. However, it should be noted that more experimental or theoretical work is needed to finally clarify the apparently complex solution behavior of these compounds.

The equatorial ligands are most likely fluxional in both cases down to −80 °C, finally resulting in the observed intensity ratio of 2:6 (1:3). This suggestion is also supported by the molecular structure of the trinuclear compound Pd_3Al_6 (**3**), bearing two axial and four equatorial ligands. The equatorial ligands in **3** are fluxional in solution down to −80 °C (vide supra).

Thermodynamic and kinetic considerations: Thermodynamically, the substitution of coordinated GaCp* in M_2Ga_5 by AlCp*, PPh_3, CO, or isonitriles appears to be a favorable reaction, since in all cases investigated, either full or partial ligand exchange was observed. The π-acceptors CO, isonitriles, and PPh_3 were found in a terminal positions of the dinuclear clusters, whereas the remaining ECp* prefer the bridging positions. Interestingly, AlCp* favors the bridging position in direct competition with GaCp* in the case of $Pt_2Al_3Ga_2$ (**1d**). This may be due to the stronger σ-donor properties of AlCp*. In general, the AlCp*-containing dinuclear clusters Pd_2Al_5 (**1e**) and $Pt_2Al_3Ga_2$ (**1d**) do not undergo further substitution reactions with phosphines, confirming the higher bond strength of M−Al in the first place.

In virtually all substitution reactions of M_2E_5, the nuclearity of the M_2 core was retained. Taking the fact into account that all monomeric compounds ME_4 are kinetically inert and that none of the clusters M_2E_5 or M_3E_n ($n=6$, 8) forms monomers in the presence of an excess of free ECp*, it can be assumed that a high kinetic barrier prevents the dimeric cluster from breaking into two monomers.

Still, the origin of the kinetic activity of the dimeric clusters M_2E_5 in ligand exchange reactions has to be addressed. As both metal centers in M_2E_5 are sterically saturated (tetrahedral environment), a dissociative mechanism, with respect to bridging ligands, for the substitution reactions as well as the fluxional processes seems most reasonable (Scheme 5). The intermediate is supposedly equal for both processes, as is reflected by the same qualitative trend in the rates of fluxionality and reactivity (as indicated by variable-temperature NMR measurements). This intermediate is probably formed by the rupture of one bridging M−E bond and thus exhibits a coordinatively-unsaturated transition metal, which is likely to be the reactive center for the incoming ligands in the subsequent associative substitution reactions. The nature of the saturated transition-metal center in this intermediate, now having two equivalent terminal ligands, can well explain the exchange process of terminal and bridging ligands. The fact that ME_4 clusters are kinetically inert in contrast to M_2E_5 could be reasoned by taking into account that splitting only one M−E connectivity in the case of the M_2E_5 unit is of course likely to cost less activation energy per M_2E_5 molecule than complete dissociation of ME_4 in ME_3 and free E. This situation is comparable to the well-studied classical metal–carbonyl cluster complexes, with the terminally bound carbonyls generally being less reactive than the bridging ones.[26,27]

The relative inertness of $Pt_2Al_3Ga_2$ (**1d**) in the presence of phosphines is in agreement with this mechanism, as the rupture of the M−E bond of the bridging AlCp* ligand would require more energy in comparison to the bridging GaCp* unit in the related Pt_2Ga_5 (**1a**). However, reaction of $Pt_2Al_3Ga_2$ (**1d**) with CO does lead to $[Pt_2(CO)_2(\mu_2\text{-AlCp*})_3]$ over a period of two days at room temperature. In contrast, Pt_2Ga_5 (**1a**) reacts with CO under ambient conditions within a couple of minutes giving $[Pt_2(CO)_2(\mu_2\text{-GaCp*})_3]$ (**6**).[28]

Finally, it should be noted here, that we probably misinterpreted the fluxionality of the trimetallic complex $PtPdGa_5$ (**1b**) in the original publication.[14] Taking the proposed mechanism above into account, the fluxional terminal GaCp* ligand should actually be bound to the platinum center rather than the palladium center, as the Pd−Ga bonds should be weaker than the Pt−Ga bonds, thus creating a symmetric saturated platinum rather than palladium center in the intermediate.

Conclusion

In this work we have presented a general and direct route to a variety of homoleptic, mixed-metal clusters with di- and trinuclear palladium and platinum cores and ECp* (E = Al, Ga, In) as stabilizing ligands. The formation of these clusters is determined by kinetic factors, and clusters with different nuclearity are not interconvertible to each other by addition of free ligand. The reactivity of M_2E_5 and M_3E_8 towards ligand substitution was studied in some detail. A qualitative relationship between rates of fluxional processes and ligand-substitution reactions was established, resulting in mechanistic suggestions for both. The triangular nature of the substitution products of M_3E_8 leads to a better understanding of the NMR spectroscopic features

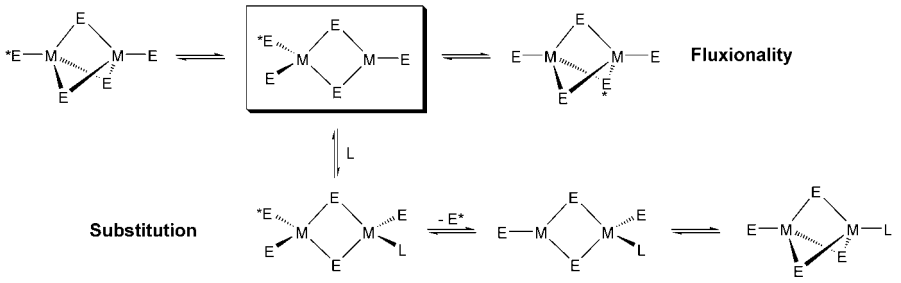

Scheme 5. Proposed mechanism for the substitution reactions as well as the fluxional processes of $[M_2(ECp^*)_5]$ (M = Pd, Pt).

and thus the molecular structures of M_3E_8 in solution, which have a triangular rather than a linear arrangement of the transition-metal centers as found in the solid state. The kinetic accessibility of the formally unsaturated M_2E_5 and M_3E_8 clusters in contrast to the saturated ME_4 systems may allow interesting chemistry, such as activation of small molecules similar to the case of the unsaturated intermediate [Ni(AlCp*)$_3$] presented previously,[15] or the unusual C–C bond activation observed in the rearrangement of [Rh(Cp*)(CH$_3$)$_2$(GaCp*)] to the zwitterionic product [Rh(Cp*){η^5-C$_5$Me$_4$(Ga(CH$_3$)$_3$)}].[34] We will report on the further development of this chemistry, in particular with respect to other d-block metals and complexes of higher and as well lower coordination numbers than reported here in due course.[28,29]

Experimental Section

All manipulations were carried out in an atmosphere of purified argon using standard Schlenk and glove box techniques. Hexane, toluene, THF and Et$_2$O were dried using an MBraun Solvent Purification System, all other solvents were dried by distillation over standard drying agents. The final H$_2$O content in all solvents used was checked by Karl–Fischer-titration and did not exceed 5 ppm. [Pd$_2$(dvds)$_3$],[30] AlCp*,[31,32] and GaCp*[33] were prepared according to recent literature methods. Elemental analyses were performed by the Microanalytical Laboratory of the Ruhr-Universität Bochum. Melting or decomposition points were determined thermogravimetrically on a Seiko EXSTAR 6300S11 TG/DTA instrument. NMR spectra were recorded on a Bruker Avance DPX-250 spectrometer (^{1}H, 250.1 MHz; ^{13}C, 62.9 MHz) in C$_6$D$_6$ at 298 K unless otherwise stated. Chemical shifts are given relative to TMS and were referenced to the solvent resonances as internal standards.

The crystal structures of **1c**, **1e**, **2b**, and **4b** were measured on a SMART CCD1000 diffractometer, the structures of **1d**, **3**, **4a**, and **8** were measured on an Oxford Excalibur 2 diffractometer with $Mo_{K\alpha}$ radiation (λ = 0.71073 Å). The structures were solved by direct methods by using SHELXS-97 and refined against F^2 on all data by full-matrix least-squares with SHELXL-97. Details of the measurements are given in Table 7.

CCDC-250431 (**1c**), CCDC-250432 (**1d**), CCDC-250433 (**1e**), CCDC-250434 (**2b**), CCDC-250435 (**3**), CCDC-250436 (**4a**), CCDC-250437 (**4b**), CCDC-250438 (**8**) contains the supplementary crystallographic data for this paper. These data can be obtained free of charge from The Cambridge Crystallographic Data Centre via www.ccdc.cam.ac.uk/data_request/cif.

[Pd$_2$(GaCp*)$_2$(μ_2-GaCp*)$_3$] (1c): [Pd$_2$(dvds)$_3$] (0.800 g, 1.036 mmol) in hexane (5 mL) was cooled to −30 °C and treated dropwise with GaCp* (1.272 g, 6.218 mmol). The resulting orange solution was slowly warmed to room temperature, whereupon an orange precipitate was formed. The product was isolated by means of cannulation, washed twice with a small amount of cold hexane and dried in vacuo. The precipitate was dissolved in toluene and the product crystallized by slow cooling to −30 °C. In trace amounts (<3 %) the monomeric compound [Pd(GaCp*)$_4$] was observed. Yield: 1.211 g (94 %); m.p. 118 °C (decomp); ^{1}H NMR (C$_6$D$_6$, 250 MHz, 25 °C): δ = 1.98 ppm (s, 75 H); ^{13}C NMR (C$_6$D$_6$, 62.9 MHz, 25 °C): δ = 113.3 (*C*$_5$Me$_5$), 10.8 ppm (C$_5$*Me*$_5$); elemental analysis calcd (%) for C$_{50}$H$_{75}$Ga$_5$Pd$_2$: C 48.53, H 6.11; found: C 48.26, H 6.32.

[Pt$_2$(GaCp*)$_2$(μ_2-AlCp*)$_3$] (1d): A suspension of **1a** (0.250 g, 0.177 mmol) and [{AlCp*}$_4$] (0.085 g, 0.133 mmol) in toluene (5 mL) was warmed to 80 °C for 1 h. The red solution was cooled to room temperature and the product crystallized by slow cooling to −30 °C. Yield: 0.186 g (83 %); m.p. 176 °C (decomp); ^{1}H NMR (C$_6$D$_6$, 250 MHz, 25 °C): δ = 2.07 (s, 30 H), 1.86 ppm (s, 45 H); ^{13}C NMR (C$_6$D$_6$, 62.9 MHz, 25 °C): δ = 114.2 (*C*$_5$Me$_5$), 112.5 (*C*$_5$Me$_5$), 13.4 (C$_5$*Me*$_5$), 10.6 ppm (C$_5$*Me*$_5$); ^{27}Al NMR (C$_6$D$_6$, 65.2 MHz, 25 °C): δ = − 91.8 ppm; elemental analysis calcd (%) for C$_{50}$H$_{75}$Al$_3$Ga$_2$Pt$_2$: C 46.68, H 5.88; found: C 46.22, H 5.52.

[Pd$_2$(AlCp*)$_2$(μ_2-AlCp*)$_3$] (1e): A suspension of **1c** (0.250 g, 0.202 mmol) and [{AlCp*}$_4$] (0.090 g, 0.253 mmol) in toluene (7 mL) was warmed to 85 °C for 3 h. The pale-orange solution turned red and a red–brown precipitate was formed. After removal of all volatiles in vacuo, the residue was washed twice with cold hexane and dried in vacuo. The precipitate was dissolved in toluene by warming to 90 °C and the product crystallized by slow cooling to −30 °C. Yield: 0.162 g (78 %); m.p. 204 °C (decomp); ^{1}H NMR (C$_6$D$_6$, 250 MHz, 25 °C): δ = 2.00 (s, 30 H), 1.94 ppm (s, 45 H); ^{13}C NMR (C$_6$D$_6$, 62.9 MHz, 25 °C): δ = 113.9 (*C*$_5$Me$_5$), 112.8 (*C*$_5$Me$_5$), 12.5 (C$_5$*Me*$_5$), 10.6 ppm (C$_5$*Me*$_5$); ^{27}Al NMR (C$_6$D$_6$, 65.2 MHz, 25 °C): δ = −54.4 ppm; elemental analysis calcd (%) for C$_{50}$H$_{75}$Al$_5$Pd$_2$: C 58.94, H 7.42; found: C 58.92, H 7.66.

[Pd$_3$(InCp*)$_4$(μ_2-InCp*)$_4$] (2a): [Pd$_2$(dvds)$_3$] (0.500 g, 0.648 mmol) in toluene (5 mL) was treated with InCp* (1.133 g, 4.534 mmol) at 50 °C, whereupon the color of the solution turned dark red and a red precipitate was formed. After removal of all volatiles in vacuo, the residue was washed twice with cold hexane and dried in vacuo. Yield: 0.874 g (88 %). All analytical data were in good agreement with the data reported.[8]

[Pd$_3$(GaCp*)$_4$(μ_2-GaCp*)$_4$] (2b): [Pd$_2$(dvds)$_3$] (0.500 g, 0.648 mmol) in toluene (5 mL) was treated dropwise with Cp*Ga (0.927 g, 4.534 mmol), whereupon a red precipitate was formed. The product was isolated by means of cannulation, washed twice with a small amount of hexane, and dried in vacuo. The precipitate was dissolved in toluene by warming to 90 °C and the product crystallized by slow cooling to −30 °C. In trace amounts (<2 %) the dimeric compound [Pd$_2$(GaCp*)$_5$] was observed. Yield: 0.651 g (76 %); m.p. 178 °C (decomp); ^{1}H NMR (C$_6$D$_6$, 250 MHz, 25 °C): δ = 2.05 (s, 15 H), 1.96 ppm (s, 45 H); ^{13}C NMR (C$_6$D$_6$, 62.9 MHz, 25 °C): δ = 113.6 (*C*$_5$Me$_5$), 10.4 ppm (C$_5$*Me*$_5$); elemental analysis calcd (%) for C$_{80}$H$_{120}$Ga$_8$Pd$_3$: C 49.05, H 6.17; found: C 48.84, H 6.18.

[Pd$_3$(AlCp*)$_2$(μ_2-AlCp*)$_2$(μ_3-AlCp*)$_2$] (3): A mixture of [Pd$_2$(dvds)$_3$] (0.250 g, 0.324 mmol) and [{AlCp*}$_4$] (0.522 g, 0.809 mmol) in benzene (5 mL) was warmed to 60 °C for 1 h, whereupon the color of the solution turned dark red and a dark red–brown precipitate was formed. The product was isolated by means of cannulation, washed twice with a small amount of hexane, and dried in vacuo. The residue was dissolved in toluene by warming to 90 °C and the product crystallized by slow cooling to room temperature. Yield: 0.178 g (64 %); m.p. 196 °C (decomp); ^{1}H NMR (C$_6$D$_6$, 250 MHz, 25 °C): δ = 2.12 (s, 30 H), 1.97 ppm (s, 60 H); ^{13}C NMR (C$_6$D$_6$, 62.9 MHz, 25 °C): δ = 113.8 (*C*$_5$Me$_5$), 113.0 (*C*$_5$Me$_5$), 14.3 (C$_5$*Me*$_5$), 11.2 (C$_5$*Me*$_5$) ppm; ^{27}Al NMR (C$_6$D$_6$, 65.2 MHz, 25 °C): δ = −44.6 ppm; elemental analysis calcd (%) for C$_{60}$H$_{90}$Al$_6$Pd$_3$·C$_6$H$_5$(CH$_3$): C 58.10, H 7.13; found: C 57.87, H 7.19.

[Pt$_2$(PPh$_3$)(GaCp*)(μ_2-GaCp*)$_3$] (4a): A solution of **1a** (0.200 g, 0.141 mmol) and PPh$_3$ (0.074 g, 0.282 mmol) in toluene (6 mL) was warmed to 90 °C for 8 h. After removal of all volatiles in vacuo, the yellow precipitate was dissolved in toluene and crystallized by slow cooling to −30 °C. Yield: 0.156 g (75 %); m.p. 121 °C (decomp); ^{1}H NMR (C$_6$D$_6$, 250 MHz, 25 °C): δ = 7.75–7.10 (m, 15 H), 2.12 (s, 15 H), 1.84 ppm (s, 45 H); ^{13}C NMR (C$_6$D$_6$, 62.9 MHz, 25 °C): δ = 141.3 (d, J(P,C) = 44.2 Hz), 135.7 (d, J(P,C) = 14.5 Hz), 129.3 (d, J(P,C) = 4.8 Hz), 125.7, 114.3 (*C*$_5$Me$_5$), 112.8 (*C*$_5$Me$_5$), 11.2 (C$_5$*Me*$_5$), 10.5 ppm (C$_5$*Me*$_5$); ^{31}P{^{1}H} NMR (C$_6$D$_6$, 101.3 MHz, 25 °C): δ = 66.0 ppm (^{1}J(Pt,P) = 5685 Hz; ^{2}J(Pt,P) = 276 Hz); elemental analysis calcd (%) for C$_{58}$H$_{75}$Ga$_4$PPt$_2$: C 47.32, H 5.13; found: C 47.67, H 4.95.

[PtPd(PPh$_3$)(GaCp*)(μ_2-GaCp*)$_3$] (4b): A solution of **1b** (0.100 g, 0.075 mmol) and PPh$_3$ (0.020 g, 0.075 mmol) in toluene (3 mL) was stirred at room temperature for 1 h. After removal of all volatiles in vacuo, the yellow precipitate was dissolved in toluene and crystallized by slow cooling to −30 °C. Yield: 0.078 g (75 %); m.p. 114 °C (decomp); ^{1}H NMR (C$_6$D$_6$, 250 MHz, 25 °C): δ = 7.85–7.25 (m, 15 H), 2.11 (s, 15 H), 1.84 ppm (s, 45 H); ^{13}C NMR (C$_6$D$_6$, 62.9 MHz, 25 °C): δ = 139.1 (d, J(P,C) = 28.4 Hz), 135.3 (d, J(P,C) = 17.7 Hz), 129.3 (d, J(P,C) = 2.4 Hz), 128.1, 114.1 (*C*$_5$Me$_5$), 112.9 (*C*$_5$Me$_5$), 11.2 (C$_5$*Me*$_5$), 10.6 ppm (C$_5$*Me*$_5$); ^{31}P{^{1}H} NMR (C$_6$D$_6$, 101.3 MHz, 25 °C): δ = 53.0 ppm (t, ^{2}J(Pt,P) = 494 Hz); ele-

Table 7. Crystallographic data for compounds **1c**, **1d**, **1e**, **2b**, **3**, **4a**, **4b**, and **8**.

	1c	**1d**	**1e**	**2b**
formula	$C_{51.75}H_{77}Ga_5Pd$	$C_{50}H_{75}Al_3Ga_2Pd$	$C_{50}H_{75}Al_5Pd$	$C_{80}H_{120}Ga_8Pd_3$
M_r [g mol^{-1}]	1260.53	1286.66	1023.80	1958.72
T [K]	203(2)	103(2)	208(2)	213(2)
crystal system	triclinic	monoclinic	monoclinic	monoclinic
space group	$P\bar{1}$	$C2/c$	$C2/c$	$C2/c$
a [Å]	15.205(4)	45.097(2)	14.984(5)	31.92(5)
b [Å]	20.824(6)	11.6375(8)	20.096(6)	12.69(3)
c [Å]	20.879(6)	22.473(2)	19.032(8)	24.88(4)
α [°]	60.279(7)	90	90	90
β [°]	87.525(7)	98.326(6)	101.947(13)	118.41(5)
γ [°]	85.723(7)	90	90	90
V [Å^3]	5725(3)	11669(15)	5607(3)	8867(28)
Z	4	8	4	4
ρ_{calcd} [g cm^{-3}]	1.462	1.465	1.213	1.467
μ [mm^{-1}]	2.960	5.766	0.748	3.017
F (000)	2583	5056	2128	3944
2θ range [°]	1.13–25.31	3.12–25.07	2.19–26.15	2.15–25.06
index ranges	$-18 \le h \le 16$	$-41 \le h \le 53$	$-18 \le h \le 17$	$-37 \le h \le 36$
	$-24 \le k \le 24$	$-13 \le k \le 13$	$-23 \le k \le 23$	$-15 \le k \le 6$
	$-25 \le l \le 16$	$-26 \le l \le 20$	$-18 \le l \le 23$	$-29 \le l \le 27$
reflections collected	33260	44079	16002	11752
reflections unique	20381 ($R_{int}=0.0463$)	10322 ($R_{int}=0.0549$)	5311 ($R_{int}=0.0458$)	7567 ($R_{int}=0.0498$)
goodness-of-fit on F^2	1.051	0.929	1.059	0.962
final R indices [$I>2\sigma(I)$]	$R_1=0.0698$	$R_1=0.0359$	$R_1=0.0540$	$R_1=0.0521$
	$wR_2=0.1738$	$wR_2=0.0747$	$wR_2=0.1615$	$wR_2=0.1144$
R indices (all data)	$R_1=0.1261$	$R_1=0.0549$	$R_1=0.0784$	$R_1=0.1103$
	$wR_2=0.2021$	$wR_2=0.0795$	$wR_2=0.1839$	$wR_2=0.1354$
	3	**4a**	**4b**	**8**
formula	$C_{60}H_{90}Al_6Pd_3$	$C_{58}H_{75}Ga_4PPt_2$	$C_{58}H_{75}Ga_4PPdPt$	$C_{84}H_{90}In_3P_3Pd_3$
M_r [g mol^{-1}]	1292.40	1472.21	1383.52	1856.13
T [K]	103(2)	100(1)	203(2)	100(1)
crystal system	monoclinic	triclinic	triclinic	triclinic
space group	$C2$	$P\bar{1}$	$P\bar{1}$	$P\bar{1}$
a [Å]	18.817(5)	11.579(3)	11.577(4)	14.369(6)
b [Å]	22.799(4)	11.648(4)	11.834(3)	14.679(5)
c [Å]	48.790(5)	21.529(6)	21.723(6)	21.995(4)
α [°]	90	101.19(3)	100.549(7)	77.735(19)
β [°]	90.050(14)	96.27(2)	96.808(7)	86.52(2)
γ [°]	90	97.47(3)	97.273(7)	63.18(3)
V [Å^3]	20932(7)	2797(14)	2871(15)	4042(2)
Z	12	2	2	2
ρ_{calcd} [g cm^{-3}]	1.230	1.748	1.600	1.525
μ [mm^{-1}]	0.871	6.944	4.644	1.594
F (000)	7992	1436	1372	1848
2θ range [°]	2.74–25.07	2.58–30.07	2.15–25.06	2.72–25.05
index ranges	$-22 \le h \le 22$	$-16 \le h \le 14$	$-9 \le h \le 13$	$-17 \le h \le 17$
	$-27 \le k \le 27$	$-13 \le k \le 16$	$-13 \le k \le 14$	$-17 \le k \le 17$
	$-58 \le l \le 57$	$-28 \le l \le 30$	$-25 \le l \le 25$	$-26 \le l \le 26$
reflections collected	125967	25538	15636	54424
reflections unique	35748 ($R_{int}=0.1945$)	14256 ($R_{int}=0.0745$)	9815 ($R_{int}=0.0645$)	14271 ($R_{int}=0.1021$)
goodness-of-fit on F^2	0.851	1.071	0.954	1.006
final R indices [$I>2\sigma(I)$]	$R_1=0.0836$	$R_1=0.0905$	$R_1=0.0713$	$R_1=0.0546$
	$wR_2=0.1320$	$wR_2=0.2089$	$wR_2=0.1784$	$wR_2=0.1159$
R indices (all data)	$R_1=0.1575$	$R_1=0.1229$	$R_1=0.1115$	$R_1=0.1102$
	$wR_2=0.1560$	$wR_2=0.2227$	$wR_2=0.1991$	$wR_2=0.1329$

mental analysis calcd (%) for $C_{58}H_{75}Ga_4PPdPt$: C 50.35, H 5.46; found: C 50.02, H 5.24.

$[Pd_2(PPh_3)_2(\mu_2\text{-GaCp*})_3]$ (5): A solution of **1c** (0.100 g, 0.081 mmol) and PPh_3 (0.042 g, 0.161 mmol) in toluene (3 mL) was warmed to 40 °C for 1 h. After removal of all volatiles in vacuo, the precipitate was washed with a small amount of hexane. The product was dissolved in toluene by warming to 80 °C and crystallized by slow cooling to −30 °C. Yield: 0.089 g (82 %); m.p. 119 °C (decomp); ^{1}H NMR (C_6D_6, 250 MHz, 25 °C): $\delta = 7.85$–7.05 (m, 30 H), 1.77 ppm (s, 45 H); ^{13}C NMR (C_6D_6, 62.9 MHz, 25 °C): $\delta = 135.5$ (d, J(P,C) = 8.4 Hz), 135.4 (d, J(P,C) = 9.0 Hz), 129.3 (d, J(P,C) = 2.4 Hz), 127.2, 113.9 (C_5Me_5), 10.4 ppm ($C_5\mathit{Me}_5$); ^{31}P{^{1}H} NMR (C_6D_6, 101.3 MHz, 25 °C): $\delta = 34.8$ ppm; elemental analysis calcd (%) for $C_{66}H_{75}Ga_4P_2Pd_2$: C 58.62, H 5.59; found: C 58.71, H 5.69.

$[Pt_2(CO)_2(\mu_2\text{-GaCp*})_3]$ (6): A mixture of a solution of **1a** (0.020 g, 0.014 mmol) in C_6D_6 (0.6 mL) and 450 mbar CO was reacted in a sealed NMR tube at room temperature for 10 min. The reaction was complete

according to the ^{1}H NMR spectrum. Isolation of the product by means of evaporation of all volatiles in vacuo or under normal pressure led to decomposition of the product. The formation of metallic platinum was detected. ^{1}H NMR (C_6D_6, 250 MHz, 25 °C): $\delta = 1.85$ ppm (s, 45 H); ^{13}C NMR (C_6D_6, 62.9 MHz, 25 °C): $\delta = 209.6$ (CO), 113.9 (C_5Me_5) 10.2 ppm (C_5Me_5); IR (C_6D_6): $\nu = 1962$ cm^{-1} (vs, CO).

[Pt$_2$(CN*t*Bu)$_2$(μ_2-GaCp*)$_3$] (7): A red solution of **1a** (0.200 g, 0.141 mmol) and *t*BuNC (0.047 g, 0.565 mmol) in toluene (3 mL) was warmed to 60 °C for 1 h. After removal of all volatiles in vacuo, the yellow precipitate was dissolved in hexane and crystallized by slow cooling to −30 °C. Yield: 0.158 g (95 %); m.p. 192 °C (decomp); ^{1}H NMR (C_6D_6, 250 MHz, 25 °C): $\delta = 2.05$ (s, 45 H), 1.14 ppm (s, 18 H); ^{13}C NMR (C_6D_6, 62.9 MHz, 25 °C): $\delta = 175.1$ (*C*NCMe$_3$), 113.1 (C_5Me$_5$), 54.6 (CN*C*Me$_3$), 30.7 (CNC*Me*$_3$), 10.8 ppm (C_5Me_5); elemental analysis calcd (%) for $C_{40}H_{63}Ga_3N_2Pt_2$: C 41.02, H 5.42, N 2.39; found: C 40.92, H 5.77, N 2.39.

[Pd$_3$(PPh$_3$)$_3$(μ_2-InCp*)(μ_3-InCp*)$_2$] (8): A mixture of **2a** (0.200 g, 0.086 mmol) and PPh_3 (0.090 g, 0.344 mmol) in toluene (3 mL) was stirred for 20 min. The solvent was removed in vacuo and the oily residue was washed twice with a small amount of hexane and dried in vacuo. The orange product was crystallized in a mixture of toluene and hexane. Yield: 0.109 g (68 %); m.p. 112 °C (decomp); ^{1}H NMR (C_6D_6, 250 MHz, 25 °C): $\delta = 7.85$–7.35 (m, 45 H), 2.11 (s, 15 H), 1.70 ppm (s, 30 H); ^{13}C NMR (C_6D_6, 62.9 MHz, 25 °C): $\delta = 140.4$ (d, J(P-C) = 13.4 Hz), 140.2 (d, J(P-C) = 13.9 Hz), 139.6, 139.2, 135.3 (d, J(P,C) = 7.9 Hz), 135.0 (d, J(P,C) = 8.2 Hz), 129.1 (d, J(P,C) = 6.4 Hz), 114.1 (C_5Me$_5$), 113.7 (C_5Me$_5$), 11.1 (C_5Me_5), 10.9 ppm (C_5Me_5); ^{31}P{^{1}H} NMR (C_6D_6, 101.3 MHz, 25 °C): $\delta = 30.3$, 13.6 ppm; elemental analysis calcd (%) for $C_{84}H_{90}In_3P_3Pd_3$: C 54.36, H 4.89; found: C 54.46, H 4.96.

[Pd$_3$(dppe)$_2$(μ_2-InCp*)(μ_3-InCp*)$_2$] (9): A mixture of **2a** (0.200 g, 0.086 mmol) and dppe (0.085 g, 0.215 mmol) in toluene (3 mL) was stirred for 1 h, whereupon an orange precipitate was formed. The solvent was removed in vacuo, and the residue was washed twice with a small amount of hexane and dried in vacuo. The product was crystallized by slow cooling a toluene solution from 90 °C to room temperature. Yield: 0.113 g (70 %); m.p. 205 °C (decomp); ^{1}H NMR (C_6D_6, 250 MHz, 25 °C): $\delta = 7.85$–7.00 (m, 40 H), 2.54 (s, 15 H), 2.10 (s, 8 H), 1.67 ppm (s, 30 H); ^{13}C NMR (C_6D_6, 62.9 MHz, 25 °C): $\delta = 129.3$, 129.1, 128.5, 125.7, 114.1 (C_5Me$_5$), 113.6 (C_5Me$_5$), 21.4 (CH$_2$), 11.8 (C_5Me_5), 11.0 ppm (C_5Me_5); ^{31}P{^{1}H}-NMR (C_6D_6, 101.3 MHz, 25 °C): $\delta = 28.4$ (^3J(P,P) = 24.3 Hz), 20.9 ppm (^3J(P,P) = 24.6 Hz); elemental analysis calcd (%) for $C_{78}H_{85}In_3P_4Pd_3$: C 51.76, H 4.73; found: C 51.94, H 4.87.

[1] C. Gemel, T. Steinke, M. Cokoja, A. Kempter, R. A. Fischer, *Eur. J. Inorg. Chem.* **2004**, 4161–4176.
[2] R. A. Fischer, J. Weiss, *Angew. Chem.* **1999**, *111*, 3002–3022; *Angew. Chem. Int. Ed.* **1999**, *38*, 2830–2850.
[3] R. Murugavel, V. Chandrasekhar, *Angew. Chem.* **1999**, *111*, 1289–1293; *Angew. Chem. Int. Ed.* **1999**, *38*, 1211–1215.
[4] W. Uhl, M. Pohlmann, R. Wartchow, *Angew. Chem.* **1998**, *110*, 1007–1009; *Angew. Chem. Int. Ed. Engl.* **1998**, *37*, 961–963.
[5] W. Uhl, S. Melle, *Z. Allg. Anorg. Chem.* **2000**, *626*, 2043–2045.
[6] P. Jutzi, B. Neumann, L. O. Schebaum, A. Stammler, H.-G. Stammler, *Organometallics* **1999**, *18*, 4462–4464.
[7] D. Weiss, M. Winter, R. A. Fischer, C. Yu, K. Wichmann, G. Frenking, *Chem. Commun.* **2000**, 2495–2496.
[8] T. Steinke, C. Gemel, M. Winter, R. A. Fischer, *Angew. Chem.* **2002**, *114*, 4955–4957; *Angew. Chem. Int. Ed.* **2002**, *41*, 4761–4763.
[9] a) J. Uddin, C. Boehme, G. Frenking, *J. Am. Chem. Soc.* **2000**, *122*, 571–582; b) R. A. Fischer, M. M. Schulte, J. Weiss, L. Zsolnai, A. Jacobi, G. Huttner, G. Frenking, C. Boehme, S. F. Vyboishchikov, *J. Am. Chem. Soc.* **1998**, *120*, 1237–1248.
[10] J. Uddin, G. Frenking, *J. Am. Chem. Soc.* **2001**, *123*, 1683–1693.
[11] M. Cokoja, C. Gemel, T. Steinke, F. Schroeder, R. A. Fischer, *Dalton Trans.* **2005**, 44–54.
[12] T. Steinke, C. Gemel, M. Cokoja, M. Winter, R. A. Fischer, *Chem. Commun.* **2003**, 1066–1067.
[13] T. Steinke, C. Gemel, M. Cokoja, R. A. Fischer, *Dalton Trans.* **2005**, 55–62.
[14] C. Gemel, T. Steinke, D. Weiss, M. Cokoja, M. Winter, R. A. Fischer, *Organometallics* **2003**, *22*, 2705–2710.
[15] T. Steinke, C. Gemel, M. Cokoja, M. Winter, R. A. Fischer, *Angew. Chem.* **2004**, *116*, 2349–2352; *Angew. Chem. Int. Ed.* **2004**, *43*, 2299–2302.
[16] J. Vollet, J. R. Hartig, H. Schnöckel, *Angew. Chem.* **2004**, *116*, 3248–3252; *Angew. Chem. Int. Ed.* **2004**, *43*, 3186–3189.
[17] W. Uhl, M. Benter, S. Melle, W. Saak, G. Frenking, J. Uddin, *Organometallics* **1999**, *18*, 3778–3780.
[18] A. Haaland, K.-G. Martinsen, H. V. Volden, D. Loos, H. Schnöckel, *Acta Chem. Scand.* **1994**, *48*, 172–174.
[19] A. Haaland, K.-G. Martinsen, S. A. Shlykov, H. V. Volden, C. Dohmeier, H. Schnöckel, *Organometallics* **1995**, *14*, 3116–3119.
[20] Q. Yu, A. Purath, A. Donchev, H. Schnöckel, *J. Organomet. Chem.* **1999**, *584*, 94–97.
[21] J. Weiss, D. Stetzkamp, B. Nuber, R. A. Fischer, C. Boehme, G. Frenking, *Angew. Chem.* **1997**, *109*, 95–97; *Angew. Chem. Int. Ed. Engl.* **1997**, *36*, 70–72.
[22] This compound emphasizes the carbenoid character of AlCp* and can be described as a twofold coordinated adduct of AlCp* to the two C=C double bonds of the dvds ligand. Analogous olefin adducts of Al^I (cycloaddition) were recently synthesized and characterized in the literature. a) C. Cui, S. Köpke, R. Herbst-Irmer, H. W. Roesky, M. Noltemeyer, H.-G. Schmidt, B. Wrackmeyer, *J. Am. Chem. Soc.* **2001**, *123*, 9091–9098; b) H. Schnöckel, M. Leimkühler, R. Lotz, R. Mattes, *Angew. Chem.* **1986**, *98*, 929–930; *Angew. Chem. Int. Ed. Engl.* **1986**, *25*, 921–922. The AlCp* units are bridging the C=C double bonds, resulting in a nine-membered [3.3.1]bicyclic system. [(dvds)(μ_2-Cp*Al)$_2$] is also obtained in the reaction of free dvds with two equivalents of Cp*Al without the presence of Pd.
[23] V. S. Segienko, M. A. Porai-Koshits, *Zh. Strukt. Khim.* **1987**, *28*, 103.
[24] D. Weiss, T. Steinke, M. Winter, R. A. Fischer, N. Fröhlich, J. Uddin, G. Frenking, *Organometallics* **2000**, *19*, 4583–4588.
[25] D. Weiss, M. Winter, K. Merz, A. Knüfer, R. A. Fischer, N. Fröhlich, G. Frenking, *Polyhedron* **2002**, *21*, 535–542.
[26] L. J. Farrugia, *J. Chem. Soc. Dalton Trans.* **1997**, 1783–1792.
[27] R. D. Adams, B. Captain, W. Fu, P. J. Pellechia, *Inorg. Chem.* **2003**, *42*, 3111–3118.
[28] T. Steinke, Ph.D. Thesis, Ruhr Universität Bochum **2004**.
[29] A. Kempter, Diploma thesis, Ruhr University Bochum **2004**.
[30] J. Krause, G. Cestaric, K.-J. Haak, K. Seevogel, W. Storm, K.-R. Pörschke, *J. Am. Chem. Soc.* **1999**, *121*, 9807–9823.
[31] M. Schormann, K. S. Klimek, H. Hatop, S. P. Varkey, H. W. Roesky, C. Lehmann, C. Röpken, R. Herbst-Irmer, M. Noltemeyer, *J. Solid State Chem.* **2001**, *162*, 225–236.
[32] S. Schulz, H. W. Roesky, H. J. Koch, G. M. Sheldrick, D. Stalke, A. Kuhn, *Angew. Chem.* **1993**, *105*, 1828–1830; *Angew. Chem. Int. Ed. Engl.* **1993**, *32*, 1729–1731.
[33] P. Jutzi, L. O. Schebaum, *J. Organomet. Chem.* **2002**, *654*, 176–179.
[34] T. Cadenbach, C. Gemel, R. Schmid, S. Block, R. A. Fischer, *Dalton Trans.* **2004**, 3171–3172..

Received: September 20, 2004
Published online: January 24, 2005